Catalysis Today 141 (2009) 130–137

Contents lists available at ScienceDirect

Catalysis Today

journal homepage: www.elsevier.com/locate/cattod

Monoalkylation of biphenyl over modified heteropoly acids: Novelty of cesium substituted dodecatungstophosphoric acid supported on hexagonal mesoporous silica☆

Ganapati D. Yadav *, Ginish George

Department of Chemical Engineering, University Institute of Chemical Technology, University of Mumbai, Matunga, Mumbai 400019, India

ARTICLE INFO

Keywords:
Friedel–Crafts alkylation
Heteropolyacids
Hexagonal mesoporous silica
Kinetics
Dodecaungstophosphoric acid

ABSTRACT

The current study reports the development of environmentally benign route for the alkylation of biphenyl with benzyl chloride for benzylbiphenyl synthesis. Cesium substituted dodecatungstophosphoric acid supported on hexagonal mesoporous silica (20% w/w $Cs_{2.5}H_{0.5}PW_{12}O_{40}$/HMS) was synthesized. This novel nanocatalyst was very active and stable without any deactivation. The catalyst is fully characterized. A systematic investigation of the effect of various operating parameters is done. Furthermore, a second order rate equation is developed to describe the reaction kinetics, which is validated with experimental results.

1. Introduction

Electrophilic aromatic substitution and in particular, Friedel–Crafts reactions require Lewis and Bronsted acid catalysts such as $AlCl_3$, $ZnCl_2$, HF, H_2SO_4, BF_3 and *p*-toluenesulfonic acid. Most of the batch processes use $AlCl_3$ as a homogeneous catalyst which is inexpensive, very reactive and is one of the most powerful Lewis acids. Unfortunately, it is difficult to handle $AlCl_3$ and similar metal halides as catalysts since they get readily hydrolyzed. Very often such catalysts are required in stoichiometric quantities. A large inventory of these materials poses health, safety and storage problems. Furthermore, the traditional route of liquid phase alkylation using mineral acids and $AlCl_3$ as catalysts suffers from the disadvantages of high capital cost, reactor corrosion, formation of by-products and the difficulty in catalyst regeneration [1]. For the development of cleaner and sustainable techniques in the chemical industry, such polluting catalytic processes need to be replaced.

In recent years, a great deal of effort has been directed towards the promotion of solid acid catalysts and several synthetic procedures have been reported. They are non-corrosive; presenting fewer disposal problems, their separation from liquid phase is much easier, which allows their repeated use. They permit the use of cheaper and non-polluting reagents, and offer several different reactor configurations [2]. In addition, physical and chemical properties of solid acids can be tailored and tuned to promote reactivity and selectivity and prolonged catalyst life.

Our laboratory has been investigating different aspects of green processes with benign solid acid catalysts, which have direct industrial relevance in refineries, petrochemicals, pharmaceuticals, rubber chemicals, dyestuff, agrochemicals, perfumery and flavour chemicals. Synergetic combinations of various heteropoly acids with inorganic supports as nanocatalysts have been successfully developed and evaluated in a number of industrially important reactions [3–17].

Heteropoly compounds are condensates of different oxyacids. Among many solid acid systems, heteropoly acids (HPAs) with Keggin anion structures have received the most attention due to their facile preparation and strong acidity. Extremely low surface area, poor stability and rapid deactivation are the major problems associated with heteropoly acids. Dodecatungstophosphoric acid (DTP) is the most stable among all HPAs and is commonly used for acid catalysis since it possesses the highest Bronsted acidity. The structure has a net (−3) charge, which requires three cations to satisfy the electro neutrality. If these cations are proton, the material functions as a Bronsted acid catalyst [3,18–20]. Attempts have been made to improve the efficiency of the HPAs by supporting on various high surface area inorganic supports and the replacement of protons with alkali metal salts.

Cesium salts of dodecatungstophosphoric acid (DTP) have been reported as superior catalysts than DTP itself, but the resulting $Cs_{2.5}H_{0.5}PW_{12}O_{40}$ (Cs-DTP) is very fine and separation of these

☆ This forms part of the Catalysis Society of India Eminent Scientist Award Lecture.

* Corresponding author. Tel.: +91 22 24102121; fax: +91 22 2414 5614.
E-mail addresses: gdyadav@yahoo.com, gdyadav@udct.org (G.D. Yadav).

0920-5861/$ – see front matter © 2008 Elsevier B.V. All rights reserved.
doi:10.1016/j.cattod.2008.04.013

Nomenclature

a_P	solid–liquid interfacial area (cm^2/cm^3 of liquid phase)
A	reactant species A, benzyl chloride
AS	chemisorbed A
B	reactant species B, biphenyl
BS	chemisorbed B
C_A, C_B	concentration of A and B (mol/cm^3)
C_{A0}, C_{B0}	initial concentration of A and B (mol/cm^3)
C_{AS}, C_{BS}	concentration of A and B at solid (catalyst) surface (mol/g cat)
C_E, C_W	concentration of E and W (mol/cm^3)
C_S	concentration of vacant sites (mol/g cat)
C_t	total concentration of the sites (mol/g cat)
C_{WP}	Weisz–Prater constant
C_{WS}, C_{ES}	concentration of W and E at solid (catalyst) surface (mol/g cat)
d_P	diameter of catalyst particle (cm)
D_{AB}	diffusion coefficient of A in B (cm^2/s)
D_{BA}	diffusion coefficient of B in A (cm^2/s)
D_e	effective diffusivity (cm^2/s)
E	benzylbiphenyl
ES, WS	chemisorbed E and W
k_{R2}	reaction rate constant (cm^6/g cat/mol/s)
$k_{SL\text{-}A}$, $k_{SL\text{-}B}$	solid–liquid mass transfer coefficients (cm/s)
k_2	dual site surface reaction rate constant (g cat/mol/s)
K_A, K_B	chemisorption equilibrium constant for A and B on catalyst surface (cm^3/mol)
K_E, K_W	chemisorption equilibrium constant for E and W on catalyst surface (cm^3/mol)
M	C_{B0}/C_{A0}
r_{obs}	observed rate of reaction (mol/g cat/s)
S	vacant site
Sh	Sherwood number
t	time (s)
w	catalyst loading (g/cm^3 of liquid phase)
W	hydrogen chloride
X_A	fractional conversion of A

Greek letters

ε	porosity
ρ_p	density of catalyst particle (g/cm^3)
τ	tortuosity

particles from reaction mixture still remains a problem [21]. Recently our group has successfully incorporated $Cs_{2.5}H_{0.5}PW_{12}O_{40}$ on to K-10 clay by in situ generation of this salt in K-10 clay [11–15]. The catalyst was found to be highly active to many industrially important reactions. As an extension to our earlier research work and to increase the surface area of the catalyst, it was thought to incorporate salt of $Cs_{2.5}H_{0.5}PW_{12}O_{40}$ in to highly ordered hexagonal mesoporous silica (HMS).

Benzylbiphenyls, particularly 4-benzylbiphenyl, are mainly used as the components of thermal recording materials and also in the field of electrophotographic photoreceptors [22,23]. Thus it was thought worthwhile to investigate the synthesis of benzylbiphenyl using cesium substituted dodecatungstophosphoric acid supported on hexagonal mesoporous silica (20% w/w $Cs_{2.5}H_{0.5}PW_{12}O_{40}$/HMS) as a catalyst, including the characterization and kinetic modeling and the findings are reported in this paper.

2. Experimental

2.1. Chemicals

The following chemicals were procured from firms of repute and used without further purification: biphenyl, benzyl chloride, cyclohexane, cesium chloride, dodecatungstophosphoric acid, ethanol (S.D. Fine Chem. Ltd., Mumbai, India), hexadecyl amine (Spectrochem. Ltd., Mumbai, India), tetraethyl orthosilicate (Fluka, Germany).

2.2. Catalyst synthesis

Hexagonal mesoporous silica was prepared as follows. 5 g hexadecyl amine was dissolved in 41.8 g of ethanol and 29.6 g of distilled water to which 20.8 g of tetraethyl orthosilicate was added under vigorous stirring. The addition of ethanol improved the solubility of the template. The mixture was aged for 18 h at 30 °C. The clear liquid above the white colored precipitate was decanted and the precipitate HMS was dried on a glass plate. The template was removed by calcining the resulting material at 550 °C in air for 3 h [24].

The catalyst was prepared by incipient wetness technique. 10 g of precalcined HMS was dried in oven at 120 °C for 3 h of which 8 g were weighed accurately. 0.2808 g (1.671×10^{-3} mol) of CsCl was weighed accurately and dissolved in 10 ml of methanol. This volume of solvent used was approximately equal to the pore volume of the catalyst. The solution was added in small aliquots of 1 ml each time to the silica molecular sieve with constant stirring with a glass rod or kneading it properly. The solution was added at time intervals of 2 min. Initially on addition of the CsCl solution to HMS was in powdery form but on complete addition it formed a paste. The paste on further kneading for 10 min resulted in a free flowing powder. The resulted material was dried at 120 °C for 3 h for the removal of solvents. This then was further subjected to impregnation by an alcoholic solution of 2 g (6.688×10^{-4} mol) of dodecatungstophosphoric acid (DTP) in 10 ml of methanol. The solution was added to the treated HMS by following the above procedure. The preformed material was dried in an oven at 120 °C for 3 h and then calcined at 300 °C for 3 h. The catalyst was found to possess highest activity when calcined at above-mentioned temperature.

2.3. Catalyst characterization

Infrared spectra of the samples pressed in KBr pellets were obtained at a resolution of 2 cm^{-1} between 4000 and 400 cm^{-1}. Spectra were collected with a Perkin-Elmer instrument and in each case the sample was referenced against a blank KBr pellet. Surface area measurements and pore size distributions analysis were done by nitrogen adsorption on Micromeritics ASAP 2010 instrument at an adsorption temperature 77 K, after pretreating the sample under high vacuum at 300 °C for 4 h. Powder X-ray diffraction (XRD) patterns were obtained using Cu Kα radiation ($\lambda = 1.540562$). Samples were step scanned from 5 to 45 in 0.045 steps with a stepping time of 0.5 s. The elemental composition of HMS and 20% (w/w) $Cs_{2.5}H_{0.5}PW_{12}O_{40}$/HMS were obtained by Energy Dispersive X-ray Spectroscopy (EDXS) on KEVEX X-ray spectrometer. Scanning electron micrographs of HMS

and 20% (w/w) $Cs_{2.5}H_{0.5}PW_{12}O_{40}$/HMS were taken on Cameca SU 30 microscope. The dried samples were mounted on specimen studs and sputter coated with a thin film of gold to prevent charging. The gold-coated surface was then scanned at various magnifications using scanning electron microscope. The ammonia-TPD data were recorded for both DTP/HMS and Cs-DTP/HMS by using AutoChem II 2920 TPD/TPR instrument (Micromeritics, USA) by using 10% NH_3 in He (Fig. 4). Also the TPR of the Cs-DTP/HMS samples was also recorded using 10% H_2 in Ar.

2.4. Reaction procedure

The reaction was carried out in a 70 ml capacity glass reactor of 3.5 cm i.d. equipped with four equally spaced baffles and six bladed turbine impeller. The reaction temperature was maintained by means of a thermostatic oil bath, which was maintained at a desired temperature with an accuracy of ±1 °C, in which the reaction assembly was immersed. Standard experiments were carried out by taking 0.03 mol biphenyl and 0.01 mol benzyl chloride in cyclohexane as solvent with a total volume of 30 cm^3, at a temperature of 80 °C, and 0.10 g/cm^3 catalyst loading. All catalysts were dried at 120 °C for 3 h before use. The reaction mixture was allowed to reach the desired temperature and the initial sample collected. Agitation was then commenced at a known speed. Samples were withdrawn periodically and analyzed by gas chromatography (GC). Typically biphenyl was taken excess and the conversions were based on the limiting reactant, benzyl chloride. The products were confirmed by GC–MS.

The reaction scheme is as shown below:

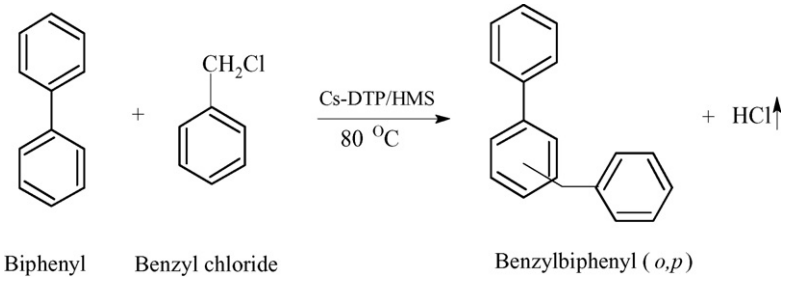

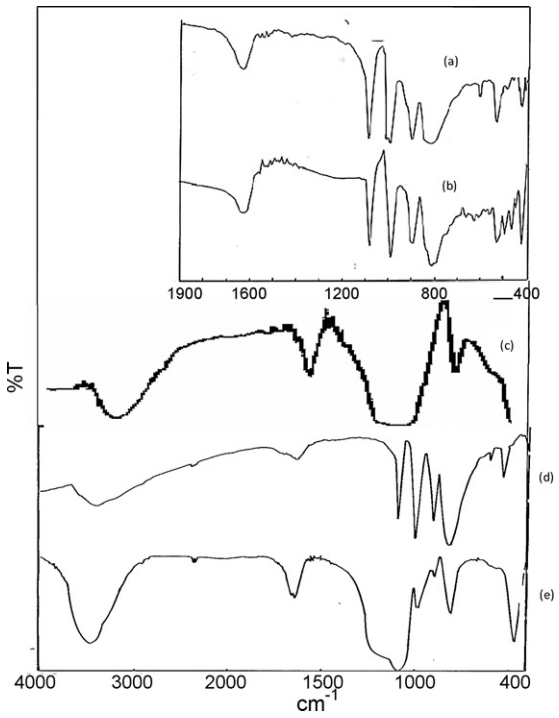

Fig. 1. FT-IR patterns of (a) Cs-DTP, (b) DTP, (c) HMS, (d) DTP/HMS, and (e) Cs-DTP/HMS (where DTP = $H_3PW_{12}O_{40}$, Cs-DTP = $Cs_{2.5}H_{0.5}PW_{12}O_{40}$).

2.5. Analysis of reaction mixture

Analysis of the reaction mixture was performed by GC (Chemito, model 8510) by using flame ionization detector and a stainless steel column (3.25 mm diameter and 4 m length) packed with a stationary phase of 10% SE-30 supported on chromosorb-WHP. Quantitative results were obtained by comparing the results with the calibration from synthetic mixtures.

3. Results and discussion

3.1. Catalyst characterization

3.1.1. FT-IR Studies

FTIR scan of bulk Cs-DTP ($Cs_{2.5}H_{0.5}PW_{12}O_{40}$) with reference to bulk DTP ($H_3PW_{12}O_{40}$) is shown in Fig. 1. Very prominent bands are observed in the region between 600 and 1000 cm^{-1}. The band at 1642 cm^{-1} is attributed to –OH bending frequency of water molecules. The FTIR scans of HMS, 20% (w/w) DTP/HMS and 20% (w/w) Cs-DTP/HMS are given in Fig. 1c–e, respectively. The IR spectrum of Cs-DTP/HMS shows typical bands at ca 1080 (P-O in the central tetrahedral), 982 (terminal W=O), 893 and 812 (W-O-W) cm^{-1} asymmetric vibrations associated with the Keggin ion. The Cs-DTP is distinctively characterized by a split in the W=O band (Fig. 1a). This doublet suggesting a direct interaction between the polyanion and Cs^+ exists [11–13,25,26]. The IR spectrum of 20% (w/w) DTP/HMS shows bands at 3450.1, 1652.6, 1092.5, 990.7, 893.4, 817.5, and 466.2 cm^{-1}. These bands coincide with those reported in the literature for the $H_3PW_{12}O_{40}$ [8,26]. The bands of the DTP-supported on HMS appear at 1092.5, 990.7 and 893.4 cm^{-1}. The presence of the 817 cm^{-1} band, in the IR spectra of supported catalytic samples, is due to a Si-O bending mode, ν_B (O-H). The sharp peak in the region 1600–1700 cm^{-1} indicates the presence of H_3O^+ (Bronsted acidity) [17]. In addition, these materials exhibit a strong 3450 cm^{-1} band which is associated with silanol group O-H stretching vibrational mode, ν_S (O-H).

3.1.2. XRD studies

The X-ray diffraction patterns of authentic HMS as well as 20% (w/w) $Cs_{2.5}H_{0.5}PW_{12}O_{40}$/HMS were recorded (not shown for sake of brevity). The XRD patterns of these materials do not contain any sharp reflections but only a broad diffuse band similar to that of amorphous materials. The XRD pattern for Cs-DTP/HMS was similar to those of the corresponding HMS. In particular, no

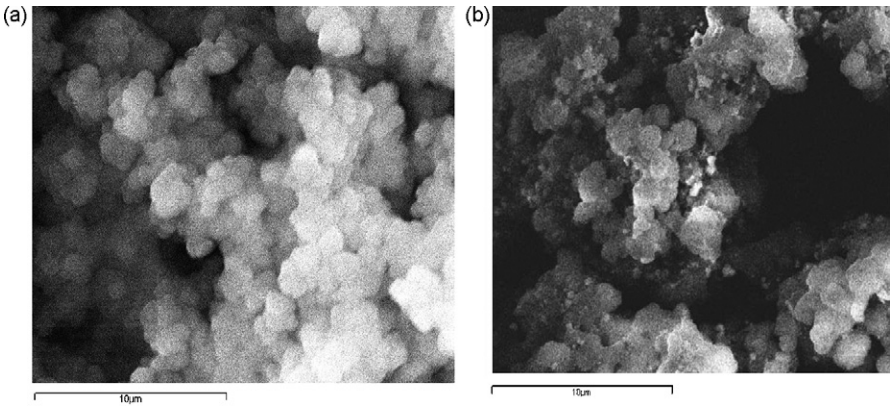

Fig. 2. SEM of HMS and 20% (w/w) $Cs_{2.5}H_{0.5}PW_{12}O_{40}$/HMS (a) HMS and (b) 20% (w/w) $Cs_{2.5}H_{0.5}PW_{12}O_{40}$/HMS.

crystalline phase could be detected in case of heteropoly acid supported on silica. This could be attributed to the uniform distribution of Keggin anion ($PW_{12}O_{40}^{3-}$) in the non-crystalline form because of the interaction with surface of silica molecular sieve. These materials are, hence, completely amorphous without any long-range order.

3.1.3. SEM and EDXS studies

The SEM images of HMS and 20% (w/w) $Cs_{2.5}H_{0.5}PW_{12}O_{40}$/HMS are shown in Fig. 2. It reveals that HMS is made up of sub-micrometer sized free standing or aggregated sphere shaped particles. Similar type of morphology is observed in the case of 20% (w/w) $Cs_{2.5}H_{0.5}PW_{12}O_{40}$/HMS. The average particle size is observed in the range of 2–4 μm. As generally observed in the case of materials synthesized by sol–gel technique, these catalytic samples show particles of irregular morphology which are fairly uniform in size. The EDXS analysis shows the presence of cesium and tungsten. SEM and EDXS analysis confirms the successful incorporation of $Cs_{2.5}H_{0.5}PW_{12}O_{40}$ in HMS pores (Table 1). Bulk DTP has a low specific surface area (<10 m^2/g). The substitution of 2.5 H^+ in DTP by 2.5 Cs^+ brought about a change in the surface area, as $Cs_{2.5}H_{0.5}PW_{12}O_{40}$ has a specific surface area value of 135 m^2/g, which is greater than bulk DTP. The particle size has decreased substantially and hence the surface area is increased. The BJH adsorption surface area of Cs-DTP/HMS is 598.8 m^2/g with average pore diameter of 3.48 nm which are correspondingly reduced from 885.9 m^2/g and 3.51 nm of the support HMS. The particles of Cs-DTP generated in situ are uniformly distributed inside the pores of HMS and are thus nano (less than average 3.51 nm of HMS). The TEM of $Cs_{2.5}H_{0.5}PW_{12}O_{40}$ also shows fine particles of the Cs-DTP.

3.1.4. Nitrogen adsorption

The textural characterization of HMS and 20% (w/w) $Cs_{2.5}H_{0.5}PW_{12}O_{40}$/HMS was determined by nitrogen BJH surface area and pore size analysis (Table 2). The nitrogen adsorption–desorption isotherm for both samples is shown in Fig. 3. For both samples, it is a type-IV isotherm, as defined by the IUPAC, with a sharp step at intermediate relative pressures. In the isotherms, three well-defined stages can be identified (i) a slow increase in nitrogen uptake at low relative pressures, corresponding to monolayer–multilayer adsorption on the pore walls, (ii) a sharp step at intermediate relative pressures indicative of capillary condensation in mesopores and (iii) a plateau at high relative pressures associated with multilayer adsorption on the external surface. Also Fig. 3a indicates that smaller channels are created inside HMS due to deposition on nanoparticles of Cs-DTP on pore surfaces. Further, the reduction in the BET surface area and pore volume of 20% (w/w) $Cs_{2.5}H_{0.5}PW_{12}O_{40}$/HMS in comparison with DTP/HMS are much more remarkable since nanoparticles of $Cs_{2.5}H_{0.5}PW_{12}O_{40}$ are generated in situ and some large particles can block a few pore junctions thereby reducing accessibility of some channels of HMS (Table 2). The pore size distribution of both HMS and Cs-DTP/HMS is also similar and that there is reduction in average pore diameter from 3.51 to 3.48 nm (Fig. 3b). This is also an indirect proof of creation of nanosize particles of Cs-DTP inside the pores of HMS.

3.1.5. TPD-TPR studies

The TPD showed that the total acidity of the sample was of Bronsted type with 477.8 and 135.3 μmol/g, respectively (Fig. 4). There is a substantial reduction in acidity on exchanging H^+ with Cs^+. Very weak signals for adsorption of H_2 on Cs-DTP/HMS, meaning no appreciable hydrogenation activity. This would suggest Cs goes in to the structure of DTP.

3.2. Catalyst activity

3.2.1. Evaluation of catalyst stability

The ordered mesoporous silica molecular sieve with large surface silanol groups is catalytically inert. The surface acidity of HMS was due to $Cs_{2.5}H_{0.5}PW_{12}O_{40}$. However, it was important to establish the exact nature of interaction between $Cs_{2.5}H_{0.5}PW_{12}O_{40}$ and silica surface. If $Cs_{2.5}H_{0.5}PW_{12}O_{40}$ was physically adsorbed on

Table 1
EDXS of HMS and 20% (w/w) $Cs_{2.5}H_{0.5}PW_{12}O_{40}$

Material	Elements	Weight (%)	Atomic (%)
HMS	O K	54.49	67.76
	Si K	45.51	32.24
	Total	100.00	
20% (w/w) $Cs_{2.5}H_{0.5}PW_{12}O_{40}$/HMS	O K	44.77	65.73
	Si K	38.22	31.97
	Cs L	2.61	0.46
	W M	14.41	1.84
	Total	100.00	

Table 2
Nitrogen BJH adsorption data of HMS and 20% (w/w) $Cs_{2.5}H_{0.5}PW_{12}O_{40}$/HMS

Material	SURFACE area (m^2/g)	Pore volume (cm^3/g)	Pore diameter (Å)
HMS	885.90	0.778	35.16
20% (w/w) $Cs_{2.5}H_{0.5}PW_{12}O_{40}$/HMS	598.81	0.522	34.86

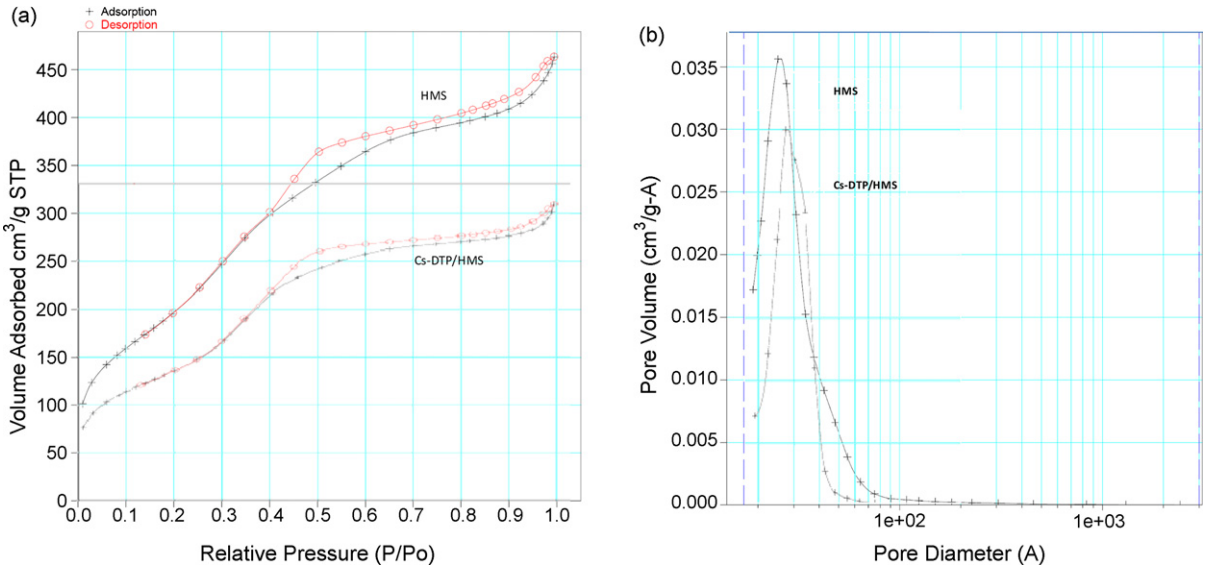

Fig. 3. (a) N_2 isotherm plots of HMS and 20% (w/w) $C_{s2.5H0.5}P_{W12O40}$/HMS, and (b) pore size distribution of HMS and 20% (w/w) $Cs_{2.5}H_{0.5}PW_{12}O_{40}$/HMS.

HMS surface, then the catalyst would not be reused because of leaching out of $Cs_{2.5}H_{0.5}PW_{12}O_{40}$ into the reaction mixture. It was observed that 20% (w/w) $Cs_{2.5}H_{0.5}PW_{12}O_{40}$/HMS showed a consistent activity up to a minimum of five runs which suggested that $Cs_{2.5}H_{0.5}PW_{12}O_{40}$ was chemically bonded to the support. For further confirmation, a typical reaction was carried out, wherein the reaction mixture consisted of 0.03 mol of biphenyl and 0.01 mol of benzyl chloride. Keeping the standard catalyst loading of 0.10 g/cm^3, the reaction was carried out at 80 °C, for 60 min. A conversion of 35% of benzyl chloride was obtained.The reaction was hot filtered and all catalyst particles were separated. The reaction was further continued at the same temperature for next 60 min without any catalyst. The sample was again analyzed to find 36.7% of benzyl chloride conversion, which is the same within the experimental error. Thus it is concluded, that the $Cs_{2.5}H_{0.5}PW_{12}O_{40}$ was chemically adsorbed on the HMS surface and the catalyst is stable.

3.2.2. Effect of speed of agitation

The effect of speed of agitation was studied in the range of 800–1200 rpm at a catalyst loading 0.10 g/cm^3 at 80 °C (Fig. 5). The mole ratio of biphenyl to benzyl chloride was kept 3:1. There was no significant change in the rate and conversion patterns, which was indicative of the absence of any resistance to external mass transfer of benzyl chloride to the external surface of the catalysts. However, all further reactions were carried out at a speed of 1000 rpm. Theoretical calculations were also done to establish that there was absence of external mass transfer resistance. We have given the theoretical development in some of our earlier work [17,26]; for instance, a typical calculation is presented here.

The rate of mass transfer could be calculated from the knowledge of mass transfer coefficients for both the reactants, which were obtained from their bulk liquid phase diffusivities. The liquid phase diffusivity values D_{AB} (benzyl chloride in cyclohexane) and D_{BA} (biphenyl in cyclohexane) were calculated by using Wilke-Chang equation. The values of D_{AB} and D_{BA} at 353 K were calculated as 6.29×10^{-5} and 6.49×10^{-5} cm^2/s, respectively. The values of solid–liquid mass transfer coefficients $k_{SL\text{-}A}$ and $k_{SL\text{-}B}$ were calculated by the Sherwood number correlation. To be on the safer side, the limiting value of the Sherwood number was taken as 2. The actual value is so far greater than 2 due to intense agitation [17].

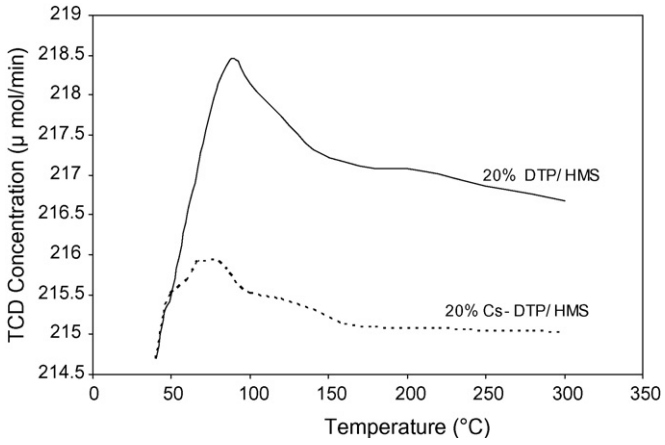

Fig. 4. Ammonia-TPD plots for 20% (w/w) $H_3PW_{12}O_{40}$/HMS and 20% (w/w) $Cs_{2.5}H_{0.5}PW_{12}O_{40}$/HMS.

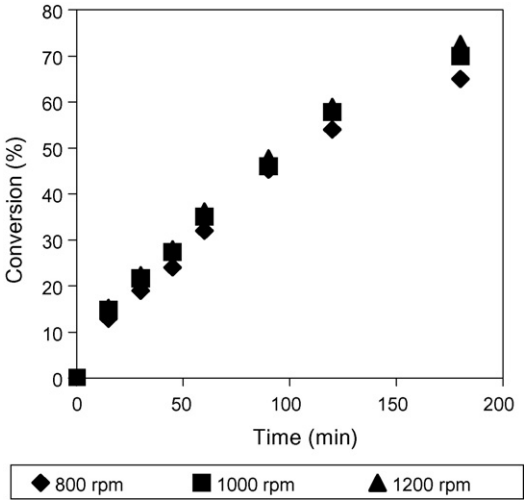

Fig. 5. Effect of speed of agitation on conversion of benzyl chloride. Conditions: biphenyl 0.03 mol, benzyl chloride 0.01 mol, total reaction volume 30 cm^3, catalyst 20% (w/w) $Cs_{2.5}H_{0.5}PW_{12}O_{40}$/HMS, catalyst loading 0.10 g/cm^3, temperature 80 °C.

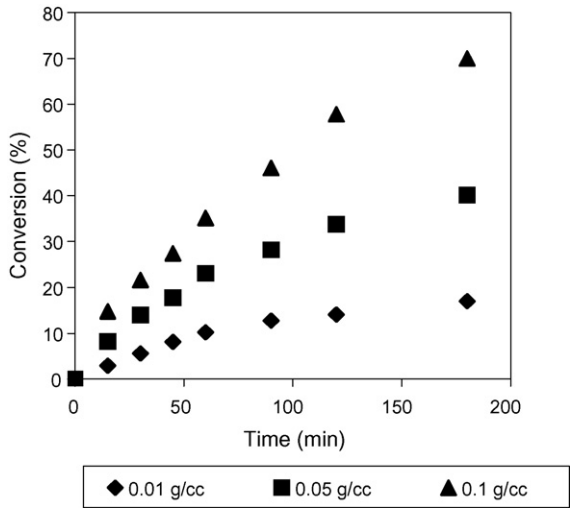

Fig. 6. Effect of catalyst loading on conversion of benzyl chloride. Conditions: 20% (w/w) $Cs_{2.5}H_{0.5}PW_{12}O_{40}$/HMS, biphenyl 0.03 mol, benzyl chloride 0.01 mol, total reaction volume 30 cm^3, temperature 80 °C, speed of agitation 1000 rpm.

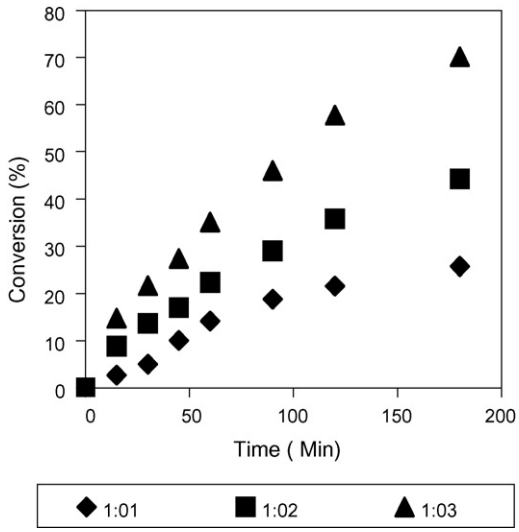

Fig. 7. Effect of mole ratio of benzyl chloride to biphenyl. Conditions: total reaction volume 30 cm^3, 20% (w/w) $Cs_{2.5}H_{0.5}PW_{12}O_{40}$/HMS, catalyst loading 0.10 g/cm^3, temperature 80 °C, speed of agitation 1000 rpm.

The values of solid–liquid mass transfer coefficients $k_{SL\text{-}A}$ and $k_{SL\text{-}B}$ were calculated by the Sherwood number correlation as 2.52×10^{-2} and 2.60×10^{-2} cm/s, respectively. The surface area of particles per unit liquid volume was calculated for 50 μm particle size (average) at a catalyst loading of 0.10 g/cm^3. Thus the values of mass transfer rates of benzyl chloride ($=k_{SL\text{-}A}a_P C_{A0}$) and biphenyl ($=k_{SL\text{-}B}a_P C_{B0}$) from the bulk liquid of the external surface of the catalyst, were found to be 2.13×10^{-3} and 6.6×10^{-3} mol/cm^3s, respectively at A:B mole ratio of 1:3. The initial observed rate of the reaction was found to be 5.37×10^{-8} mol/cm^3s. It confirms that the mass transfer rates were much higher than rates of reaction and hence speed of agitation had no influence on reaction rate.

3.2.3. Effect of catalyst loading

The effect of catalyst loading was studied over range of 0.01–0.10 g cm^{-3} (Fig. 6). In the absence of external mass transfer resistance, the rate of reaction was directly proportional to catalyst loading based on the entire liquid phase volume. This indicates that as the catalyst loading increased the conversion of benzyl chloride increases, which is due to proportional increase in the number of active sites. Further reactions were carried out with 0.10 g/cm^3 catalyst loading used in the standard reaction.

3.2.4. Effect of intra-particle diffusion resistance

The Weisz–Prater criterion was employed to assess the influence of intra-particle diffusion resistance [27,28]. According to Weisz–Prater criterion, the dimensionless parameter $\{C_{WP} = -r_{obs}\rho_p R^2{}_p/D_e[C_{AS}]\}$ which represents the ratio of the intrinsic reaction rate to the intra-particle diffusion rate, can be evaluated from the observed rate of reaction, the particle radius (R_p), effective diffusivity of the limiting reactant (D_e) and concentration of the reactant at the external surface of the particle. The effective diffusivity of benzyl chloride ($D_{e\text{-}A}$) inside the pores of the catalyst was obtained from the bulk diffusivity (D_{AB}), porosity (ε) and tortuosity (τ) as 8.38×10^{-6} cm^2/s where $D_{e\text{-}B} = D_{AB}.\ \varepsilon/\tau$. The average values of porosity and tortuosity were taken as 0.4 and 3, respectively as a conservative estimate. In the present case, the value of C_{WP} was calculated as 3.90×10^{-4}, which was less than 1, and it proved that there was no intra-particle diffusion resistance.

3.2.5. Effect of mole ratio

The effect of benzyl chloride to biphenyl mole ratio was studied at 1:1, 1:2 and 1:3 by keeping the catalyst loading constant. The conversion of benzyl chloride was found to increase with an increase in concentration of biphenyl (Fig. 7). Therefore, all reactions were studied by using a benzyl chloride: biphenyl mole ratio of 1:3.

3.2.6. Effect of temperature

The effect of temperature on conversion was studied under otherwise similar conditions at 65, 70, 75 and 80 °C, respectively. It was observed that the conversion increased with temperature (Fig. 8). This would suggest a kinetically controlled mechanism. The initial rates of reaction were calculated at different temperatures and the Arrhenius plots had made to determine the energy of activation. It was found to be 153.66 kJ/mol, which is an indication of the overall rate being controlled by intrinsic kinetics.

3.2.7. Reusability of catalyst

The reusability of the catalyst was studied by recycling the filtered and cyclohexane washed catalyst under otherwise

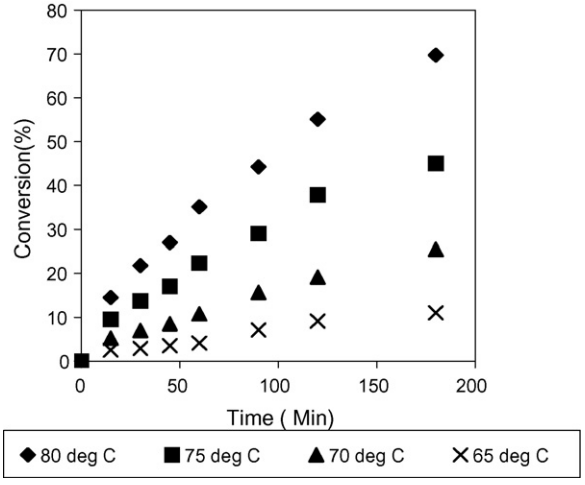

Fig. 8. Effect of temperature on conversion of benzyl chloride. Conditions: biphenyl 0.03 mol, benzyl chloride 0.01 mol, total reaction volume 30 cm^3, 20% (w/w) $Cs_{2.5}H_{0.5}PW_{12}O_{40}$/HMS, catalyst loading 0.10 g/cm^3, speed of agitation 1000 rpm.

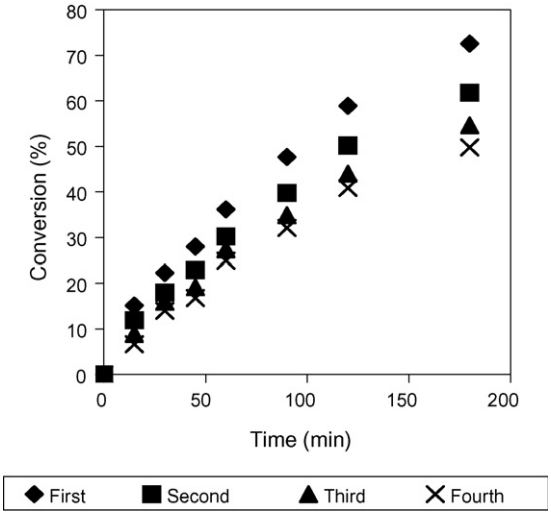

Fig. 9. Reusability of 20% (w/w) Cs-DTP/HMS. Conditions: biphenyl 0.03 mol, benzyl chloride 0.01 mol, total reaction volume 30 cm^3, catalyst loading 0.10 g/cm^3, temperature 80 °C, speed of agitation 1000 rpm.

similar conditions. The conversion had decreased from 73 to 50% from the fresh to the third reuse of the catalyst (Fig. 9). There was attrition of the catalyst; hence; some catalyst was lost during filtration. The actual amount of catalyst used in the next batch, was almost 5% less than the previous batch. The volume of the reaction mixture was adjusted to make the catalyst loading 0.10 g/cm^3, the standard value. There was only a marginal decrease in conversion. Thus, the catalyst was active and reusable.

3.2.8. Development of kinetic model

The above results were used to build a kinetic model. The reaction involves two organic phase reactants, A (benzyl chloride), B (biphenyl), the desired product E (benzylbiphenyl) and W (HCl).

Adsorption of benzyl chloride (A) on a vacant site S is given by:

$$A + S \overset{K_A}{\longleftrightarrow} AS \tag{1}$$

Similarly adsorption of biphenyl (B) on a vacant site S is given by:

$$B + S \overset{K_B}{\longleftrightarrow} BS \tag{2}$$

Surface reaction of AS and BS, in the vicinity of the site, leading to the formation of benzylbiphenyl (ES) on the site.

$$AS + BS \overset{K_2}{\longleftrightarrow} ES + WS \tag{3}$$

Desorption of benzylbiphenyl (ES) and HCl (WS) is given by:

$$ES \overset{1/K_E}{\longleftrightarrow} E + S \tag{4}$$

$$WS \overset{1/K_W}{\longleftrightarrow} W + S \tag{5}$$

The total concentration of the sites, C_t expressed as

$$C_t = C_S + C_{AS} + C_{BS} + C_{ES} + C_{WS} \tag{6}$$

or

$$C_t = C_S + K_A C_A C_S + K_B C_B C_S + K_E C_E C_S + K_W C_W C_S \tag{7}$$

or, the concentration of vacant sites,

$$C_S = \frac{C_t}{(1 + K_A C_A + K_B C_B + K_E C_E + K_W C_W)} \tag{8}$$

If the surface reaction (C) controls the rate of reaction, then the rate of reaction of A is given by

$$-r_A = -\frac{dC_A}{dt} = k_2 C_{AS} C_{BS} - k_2' C_{ES} C_{WS} \tag{9}$$

$$-\frac{dC_A}{dt} = \frac{k_2\{K_A K_B C_A C_B - (K_E K_W C_E C_W / K_2)\} C_t^2}{(1 + K_A C_A + K_E C_B + K_E C_E + K_W C_W)^2} \tag{10}$$

when the reaction is far away from equilibrium

$$-\frac{dC_A}{dt} = \frac{k_2 C_t^2 K_A K_B C_A C_B}{(1 + \sum k_i C_i)^2} \tag{11}$$

$$= \frac{k_{R2} w C_A C_B}{(1 + \sum k_i C_i)^2} \tag{12}$$

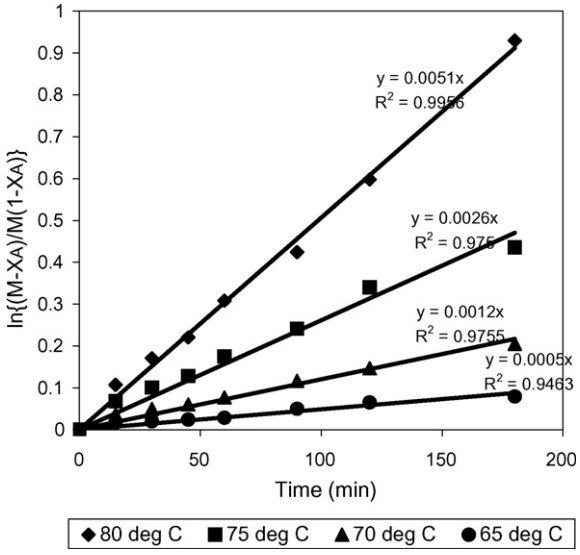

Fig. 10. Plots of $\ln\{(M - X_A)/M(1 - X_A)\}$ vs. time. Conditions: biphenyl 0.03 mol, benzyl chloride 0.01 mol, total reaction volume 30 cm^3, catalyst 20% (w/w) $Cs_{2.5}H_{0.5}PW_{12}O_{40}$/HMS, catalyst loading 0.10 g/cm^3, speed of agitation 1000 rpm.

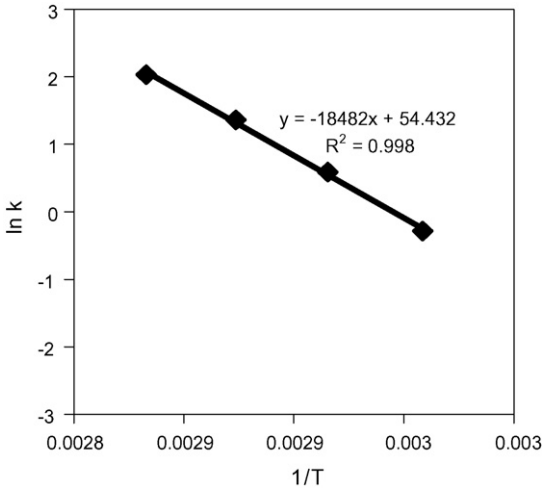

Fig. 11. Arrhenius plot of ln k vs. $1/T$.

where $k_{R2}w = k_2 C_t^2 K_A K_B$; w is catalyst loading. If the adsorption constants are very small, then the above equation reduces to

$$-\frac{dC_A}{dt} = k_{R2} C_A C_B w \quad (13)$$

Let $C_{B0}/C_{A0} = M$, the molar ratio of biphenyl to benzyl chloride at time $t = 0$. Then Eq. (13) can be written in terms of fractional conversion as

$$\frac{dX_A}{dt} = k_{R2} w C_{A0}(1 - X_A)(M - X_A) = k_1 C_{A0}(1 - X_A)(M - X_A) \quad (14)$$

this upon integration leads to:

$$\ln\left\{\left(\frac{M - X_A}{M(1 - X_A)}\right)\right\} = k_1 C_{A0}(M - 1)t$$

Thus a plot of $\ln\{(M - X_A)/M(1 - X_A)\}$ against time t was made at different temperatures to get an excellent fit, thereby supporting the model (Fig. 10). This is an overall second order reaction. The values of the rate constants at different temperatures were calculated and an Arrhenius plot was used to estimate the activation energy of the reaction (Fig. 11). The apparent activation energy was found to be 153.66 kJ/mol.

4. Conclusion

The Friedel–Crafts alkylation of biphenyl by benzyl chloride was studied systematically using 20% cesium substituted dodecatungstophosphoric acid supported on hexagonal mesoporous silica (20% $Cs_{2.5}H_{0.5}PW_{12}O_{40}$/HMS) as the catalyst. The catalyst was fully characterized. It was found to be very active, selective, stable and reusable catalyst, gives 100% selectivity towards mono alkylated product. The effects of various parameters on the rates were discussed. A second order rate equation for the reaction mechanism was successfully developed and the activation energy estimated.

Acknowledgement

GDY acknowledges support from the Darbari Seth Professor endowment and GG is grateful to the Ambuja Educational Institute, a Trust of M/s Gujarat Ambuja Cements Ltd, for bestowing financial assistance as JRF. GDY also thanks the Purdue University for inviting him as Distinguished Visiting Scholar under the President's Asian Initiative Program, which allowed him to indulge into creative pursuits.

References

[1] G.A. Olah, Friedel–Crafts Chemistry, Wiley-Interscience, New York, 1973.
[2] R.A. Sheldon, R.S. Downing, Appl. Catal. A: Gen. 189 (1999) 163.
[3] G.D. Yadav, Cat. Surveys Asia 9 (2) (2005) 117.
[4] G.D. Yadav, N. Kirthivasan, J. Chem. Soc. Chem. Commun. (1995) 203.
[5] G.D. Yadav, N. Kirthivasan, Appl. Catal. A: Gen. 154 (1997) 29.
[6] G.D. Yadav, V.V. Bokade, Appl. Catal. A: Gen. 147 (1996) 299.
[7] G.D. Yadav, M.S. Krishnan, Ind. Eng. Chem. Res. 37 (1998) 3358.
[8] G.D. Yadav, N.S. Asthana, Ind. Eng. Chem. Res. 41 (2002) 5565.
[9] G.D. Yadav, N.S. Doshi, Org. Proc. Res. Dev. 6 (2002) 263.
[10] G.D. Yadav, P. Kumar, Appl. Catal. A: Gen. 286 (2005) 61.
[11] G.D. Yadav, N.S. Asthana, V.S. Kamble, App. Catal. A: Gen. 240 (2003) 53.
[12] G.D. Yadav, N.S. Asthana, App. Catal. A: Gen. 244 (2003) 341.
[13] G.D. Yadav, N.S. Asthana, V.S. Kamble, J. Catal. 217 (1) (2003) 88.
[14] G.D. Yadav, N.S. Asthana, S.S. Salgaonkar, Clean Tech. Environ. Policy 6 (2003) 105.
[15] G.D. Yadav, S.S. Salgaonkar, N.S. Asthana, Appl. Catal. A: Gen. 265 (2004) 153.
[16] G.D. Yadav, J.J. Nair, Micropor. Mesopor. Mater. 33 (1999) 1.
[17] G.D. Yadav, H.G. Manyar, Micropor. Mesopor. Mater. 63 (2003) 85.
[18] I.V. Kozhenikov, Catal. Rev.-Sci. Eng. 37 (2) (1995) 311.
[19] T. Okuhara, N. Mizuno, M. Misono, Adv. Catal. 41 (1996) 113.
[20] M.N. Timofeeva, Appl. Catal. A: Gen. 256 (2003) 19.
[21] Y. Izumi, M. Ono, M. Kitagawa, M. Yoshida, K. Urabe, Micropor. Mater. 5 (1995) 255.
[22] S. Yamaguchi, Jpn. Kokai 268,532 (1998), to Ricoh Co., Chem. Abstr. 129 (1998) 349028.
[23] P. Beltrame, F. Demartin, G. Zuretti, Appl. Catal. A: Gen. 218 (2001) 61.
[24] P.T. Tanev, T.J. Pinnavaia, Science 267 (1995) 865.
[25] S. Choi, Y. Wang, Z. Nie, J. Liu, C.H.F. Peden, Catal. Today 55 (2000) 117.
[26] I.V. Kozhenikov, K.R. Kloetstra, A. Sinne a, H.W. Zandbergen, H. van Bekkum, J. Mol. Catal. A: Chem. 114 (1996) 287.
[27] G.D. Yadav, S. Sengupta, Org. Proc. Res. Dev. 6 (2002) 256.
[28] H.S. Fogler, Elements of Chemical Reaction Engineering, 3rd ed., Prentice-Hall, New Delhi, 1995.